

Seasonal Variability of Snow Stratigraphy and Spectral Optical Properties on Sea Ice



Eero Rinne
Finnish Institute of Marine Research
eero.rinne@fimr.fi



Christina A. Pedersen
Norwegian Polar Institute
christina@npolar.no



Sebastian Gerland
Norwegian Polar Institute
gerland@npolar.no



Marcel Nicolaus
Norwegian Polar Institute
marcel.nicolaus@npolar.no



Introduction

Optical properties of snow strongly influence the surface energy balance within the coupled atmosphere-ice-ocean system. They control the amount of solar short-wave radiation reflected at the surface (albedo), scattered and absorbed within snow, and transmitted into the sea ice and ocean water underneath.

We perform simultaneous measurements of spectral radiation and snow and sea ice properties in the Arctic based on drift stations and long term monitoring programs.

Summary

Using a setup of three TriOS Ramses sensors, a high quality time series of spectral albedo and under-ice irradiance (transmission) was recorded. The measurements cover a whole summer period, including melt onset, melt pond evolution and fall freeze up.

In order to improve the understanding of snow and sea ice thermodynamics, radiation data need to be complemented by regular snow property observations. Additional measurements on different surface types will allow to generalize our findings and identify the most relevant processes and feedback mechanisms.

The numerical snow model SNTHERM performs well in simulating snow properties on sea ice under various boundary conditions and is a valuable tool for identifying key processes.

We plan to include profile measurements of radiation measurements using different means of sensor transportation.

Studies of snow properties

Snow properties are studied with *in situ* field measurements and sampling, as well as numerical simulations.

- Field measurements of snow properties consist of:
 - ★ snow pits with systematic measurements of
 - grain size and type
 - density and liquid water content (moisture)
 - temperature
 - ★ snow thickness profiles
 - ★ snow sampling for soot content (Black Carbon) analyses
 - ★ photo documentary of snow grains and surface conditions
 - ★ additional sea ice observations (thickness, salinity, texture)



Figure 8: Measurements of snow properties in a snow pit on Arctic sea ice.

Figure 9: Show stratigraphy from snow pit observations in Kongsfjorden, Svalbard, during late spring 2003. Snow properties were classified and averaged from several sites of the same day. z=0 represents the snow-ice-interface.

Figure 10: Model grid of the 1D snow model SNTHERM. All variables are arranged in control volumes of variable thickness, representing the actual stratigraphy. The model was adapted to simulate snow on sea ice and forced in 10 min intervals with meteorological measurements.

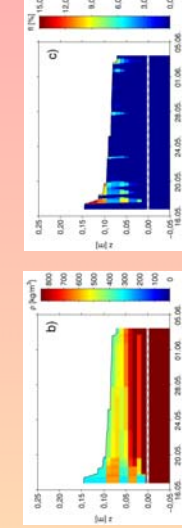


Figure 10: Model grid of the 1D snow model SNTHERM. All variables are arranged in control volumes of variable thickness, representing the actual stratigraphy. The model was adapted to simulate snow on sea ice and forced in 10 min intervals with meteorological measurements.

Snow properties are studied with *in situ* field measurements and sampling, as well as numerical simulations.

The field measurements of snow properties are complemented by numerical studies using the 1D snow model SNTHERM (Fig. 10). The field measurements of snow properties using the 1D snow model SNTHERM (Fig. 10),

simulations of different ablation seasons show that the model performs well, also when metamorphism is highest and rapid changes occur (e.g. 2003 on Svalbard, Fig. 9 and 11).

The model allows to explain observed albedo changes based on snow properties, even if *in situ* observations are sparse or not available. Especially, in combination with drift station data and monitoring programs SNTHERM is a powerful tool for radiation data interpretation.



Figure 11: Simulated snow (a) temperature, (b) density, and (c) liquid water content (2003, Kongsfjorden, Svalbard). Atmospheric forcing was taken from 2003 meteorological measurements on the ice. Snow initialization was as follows. z=0 is the snow-ice interface.

Seasonal changes of optical properties

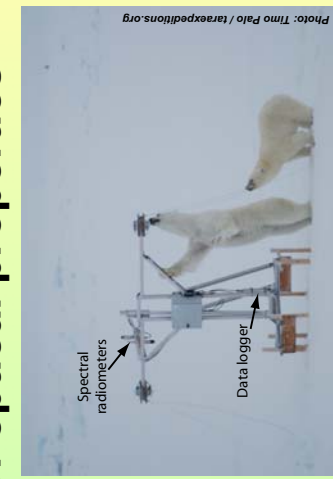


Figure 5: Measurement setup of TriOS Ramses sensors for long-term monitoring at Tara. (Left) Lowering the under-ice sensor through an ice core bore hole. (Right) The radiometer station, including broadband short- and long-wave radiometers during a visit by polar bears (05 Sep. 2007). A scheme is shown in Fig. 2.

Spectral albedo and transmission have been measured continuously (30 Apr. to 05 Sep. 2007) at the drifting schooner Tara (Fig. 1). Simultaneously snow and sea ice observations have been performed and photographs were taken regularly (Fig. 12).

- 13 June: Decrease of near-infrared albedo indicates significant snow grain size increase.

- 21 June: Decrease of albedo in visible wavelength range (compare to photos).

- 25 June: Transmission increase starts in coincidence with rapid melt pond formation. More than 15 W/m² reach the ocean under the ice.

- Mid July: Strong melt pond evolution causes decreasing albedo and a strong sea ice desalinization occurs (not shown).

- Mid August: Albedo increases much faster than the spring / summer decrease.

- Mean (integrated) albedo over the whole observation period was 0.76.

- So far, no explanation for the transmission decrease during summer can be given.

Spectral optical measurements

What to measure:

Incoming, reflected, and under-ice (transmission) spectral radiation of various surfaces (e.g. snow, sea ice, melt ponds, leads) as spot measurements or time series. Future plans include horizontal profiles of surfaces and/or under sea ice.

All radiation measurements are connected to observations of physical snow (and sea ice) properties (see right side) of different surfaces (data example, Fig. 4).

How to measure:

Two different spectral radiometer types are used:

TriOS Ramses (320-950 nm, Figs. 3, and 5) sensors are very robust and well suitable for installations to observe seasonal changes in Polar Regions. Especially under-ice irradiance is measured with the setup shown in Fig. 2.

ASD FieldSpec/pro (350-2500 nm, Fig. 3) provides a wider spectral range and a higher spectral resolution, and is therefore most suitable to characterize different surfaces (Fig. 4).

Figure 4: Spectral reflectance over different surfaces. The measurements mostly represent the deteriorated sea-ice surface, while transmission data are dominated by the melt pond (see cables to under-ice sensor).

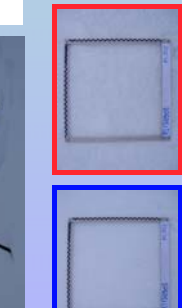
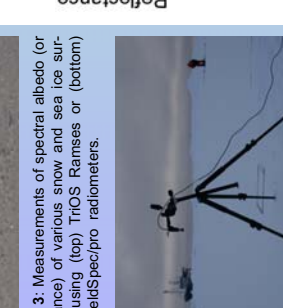
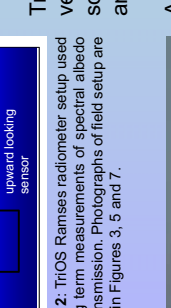
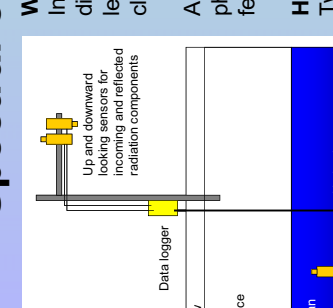


Figure 12: Photographs of the Tara monitoring area from late spring to autumn freeze up. The photos show seasonal changes of surface properties in the visible part of the solar spectrum. Especially the rapid evolution of melt ponds within one week at the end of June becomes obvious. All pictures were taken with an autonomous camera (kanukamera.com), installed on tara. The field of view is centered around the radiation station (circle in center photo). The time series ends on 22 July due to technical problems.

Figure 12: Photographs of the Tara monitoring area from late spring to autumn freeze up. The photos show seasonal changes of surface properties in the visible part of the solar spectrum. Especially the rapid evolution of melt ponds within one week at the end of June becomes obvious. All pictures were taken with an autonomous camera (kanukamera.com), installed on tara. The field of view is centered around the radiation station (circle in center photo). The time series ends on 22 July due to technical problems.

Acknowledgements

We highly appreciate the support by the Tara crew during the monitoring program. We thank R.-Jordan (CRREL) for providing the SNTHERM model. Ana Nicolaus helped preparing this poster. Presented data and results are compiled from different projects. The main part was financed by the EU-project DAMOCLES. Additional funding was received from the Norwegian Research Council (MilClim) and internal funds for various monitoring programs of the Norwegian Polar Institute.

19 July 07 08:55 UTC
07 July 07 08:30 UTC
07 June 07 08:01 UTC
25 June 07 07:31 UTC
16 May 07 04:59 UTC
30 April 07 04:01 UTC

19 July 07 08:55 UTC
07 July 07 08:30 UTC
07 June 07 08:01 UTC
25 June 07 07:31 UTC
14 June 07 07:00 UTC
07 June 07 04:59 UTC
30 April 07 04:01 UTC